# UAV-Assisted and Intelligent Reflecting Surfaces-Supported Terahertz Communications

Yijin Pan, Kezhi Wang, *Senior Member, IEEE*, Cunhua Pan, Huiling Zhu, *Senior Member, IEEE*, and Jiangzhou Wang, *Fellow, IEEE*

***Abstract*—In this letter, unmanned aerial vehicles (UAVs) and intelligent reflective surface (IRS) are utilized to support terahertz (THz) communications. To this end, the joint optimization of UAV's trajectory, the phase shift of IRS, the allocation of THz sub-bands, and the power control are investigated to maximize the minimum average achievable rate of all users. An iteration algorithm based on successive Convex Approximation with the Rate constraint penalty (CAR) is developed to obtain UAV's trajectory, and the IRS phase shift is formulated as a closed-form expression with introduced pricing factors. Simulation results show that the proposed scheme significantly enhances the rate performance of the whole system.**

***Index Terms*—Intelligent reflective surface (IRS), reconfigurable intelligent surface (RIS), terahertz (THz) communications, unmanned aerial vehicles (UAVs).**

## I. Introduction

TERAHERTZ (THz) frequency band can provide abundant bandwidth to support the ultra-high data transmission for applications such as virtual reality, etc. However, due to the ultra-high frequency, the THz links are easily blocked by obstacles on transmission paths, which makes efficient THz communications challenging.

Recently, unmanned aerial vehicles (UAVs) and intelligent reflecting surface (IRS) are leveraged for performance enhancement of wireless communications. The wireless transmission supported by the low-altitude UAV can have a better chance of line-of-sight (LoS) links with ground user equipments (UEs) due to its flexible deployment with fully-controllable mobility. However, UAV communications still face coverage and connectivity issues, especially in urban areas. UAV transmission links to UEs scattered in different locations may be still blocked by buildings and trees. Therefore, the IRS, also known as reconfigurable intelligent surface (RIS) has been proposed to help bypass obstacles in UAV systems [1]. By adjusting the phase shifts of IRS's reflecting elements, a blocked communication link can be compensated by reconfiguring the wireless propagation channels [2]. Therefore, a considerable performance gain can be obtained in the IRS-assisted and UAV-supported THz communication systems.

Many innovative efforts have been devoted to the applications of IRS in the THz transmissions. For instance, IRS was utilized in [3] to maintain reliable THz transmission, and in [4] to maximize the sum-rate performance of the THz communications. However, these approaches are mainly used for terrestrial THz communications, and they cannot be directly applied to the aerial scenario due to the flexible deployment of the UAVs. For current contributions concerning IRS assisted-UAV transmission, the UAV's trajectory, the power control, and the phase shifters of the IRS were jointly investigated in [5]. Multiple IRSs are utilized to enhance the sum-rate performance of the UAV system in [6]. Furthermore, in the THz band, severer path loss peaks appear and vary with the communication distance [7]. The THz band is composed of several sub-bands, and the previous contributions were generally designed for the single sub-band IRS-assisted UAV transmissions, so that they may not be suitable for the THz system. Although there are a few contributions on orthogonal frequency division multiplexing (OFDM) for IRS-assisted UAV systems [8], [9], these approaches were based on the specially designed simplification of conventional micro/millimeter channels, which are still not applicable to the THz communications. The path loss in THz band is severely affected by link distances, which highly rely on the trajectory of UAV. Meanwhile, the sub-bands need to be intelligently allocated to avoid the path loss peaks. Therefore, it is imperative to jointly optimize the trajectory of UAV, IRS's phase shift, along with the sub-band allocation to enhance the IRS-assisted and UAV-supported THz communication, which has not been studied in the current literature.

In this letter, we consider that the UAV supports THz communications and an IRS is deployed to help the transmission. Our aim is to maximize the minimum average rate of all UEs. To address the formulated non-convexity problem, the optimization is decoupled into three subproblems, i.e., the trajectory of UAV, the phase shift of IRS, the THz sub-band allocation and the power control optimization. Finally, simulation results are provided to validate the convergence and effectiveness of the proposed algorithm.

*Notation:* For a vector $\boldsymbol{x}$, $|\boldsymbol{x}|$ denotes its Euclidean norm. $c$ represents the light speed. $\mathrm{diag}(\boldsymbol{X})$ represents the vector that is obtained from the diagonal entries of matrix $\boldsymbol{X}$.

Manuscript received November 30, 2020; revised January 17, 2021; accepted February 28, 2021. Date of publication March 3, 2021; date of current version June 9, 2021. This work was supported in part by the National Natural Science Foundation of China under Grant 61871128, Grant 61971129, and Grant 62001107; in part by the Basic Research Project of Jiangsu Provincial Department of Science and Technology under Grant BK20190339; and in part by the U.K. Royal Society Newton International Fellowship under Grant NIF\ R1\180777. The associate editor coordinating the review of this article and approving it for publication was K. Ota. *(Corresponding author: Cunhua Pan; Kezhi Wang.)*

Yijin Pan is with the National Mobile Communications Research Laboratory, Southeast University, Nanjing 211111, China, and also with the School of Engineering and Digital Arts, University of Kent, Canterbury CT2 7NT, U.K. (e-mail: panyj@seu.edu.cn; y.pan@kent.ac.uk).

Kezhi Wang is with the Department of Computer and Information Sciences, Northumbria University, Newcastle upon Tyne NE1 8ST, U.K. (e-mail: kezhi.wang@northumbria.ac.uk).

Cunhua Pan is with the School of Electronic Engineering and Computer Science, Queen Mary University of London, London E1 4NS, U.K. (e-mail: c.pan@qmul.ac.uk).

Huiling Zhu and Jiangzhou Wang are with the School of Engineering and Digital Arts, University of Kent, Canterbury CT2 7NT, U.K. (e-mail: j.z.wang@kent.ac.uk; h.zhu@kent.ac.uk).

Digital Object Identifier 10.1109/LWC.2021.3063365

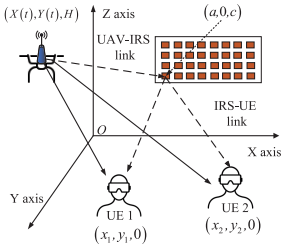


Fig. 1. IRS-assisted and UAV-supported Thz communications.

## II. System Model and Problem Formulation

Consider the downlink transmission of a UAV operating in THz frequency to serve $U$ UEs on the ground. The location of UE $u$ is denoted by $\boldsymbol{l}_u = [x_u, y_u, 0]^T$. The UAV is assumed to fly at a fixed altitude $H$ above the ground, and the total time that UAV supports communication is $T_s$. The total transmission time is divided into $T$ slots, and the location of the UAV and all channels are assumed to be unchanged within each time slot. The location of the UAV at time slot $t$ is denoted as $\boldsymbol{l}(t) = [X(t), Y(t), H]^T$.

Consider there is an IRS deployed on a wall parallel to the XOZ plane, and the IRS is assumed to be a uniform planar array (UPA). Let $N_x$ and $N_z$ respectively represent the number of reflecting elements along the $X$-axis and $Z$-axis of the IRS, and the total number of reflecting elements is $N = N_x N_z$. The separations between the elements along the $X$-axis and $Z$-axis are represented by $\delta_x$ and $\delta_z$, respectively. For the IRS, the location of its first reflecting element is denoted as $\boldsymbol{l}_0 = [a, 0, b]^T$. Then, the location of the $(n_x, n_z)$-th element of IRS is denoted by $[a+(n_x-1)\delta_x, 0, b+(n_z-1)\delta_z]^T$. Suppose that the reflection coefficients of all reflecting elements have the same amplitude value of *1* but different phase shifts. We use $\phi_n(t)$ to represent the phase shift of the $(n_x, n_z)$-th reflecting element at time slot $t$, where $n = n_z + (n_x - 1)N_z$.

### A. Direct Transmission Links

The distance between the UAV to UE $u$ at time slot $t$ is $d_u(t) = |\boldsymbol{l}(t) - \boldsymbol{l}_u|$. The UAV transmits signal through the THz band, which is affected by both free space spreading loss and the molecular absorption. As a result, the total bandwidth of the THz band is divided into several sub-bands to confront the frequency selective fading in THz band. Let $f_i$ denote the central frequency of the sub-band $i$, and the total number of sub-bands is denoted by $I$. The LoS channel gain from the UAV to UE $u$ on sub-band $i$ at time $t$ is denoted by

$$h_{i,u}(t) = \left(\frac{\lambda_i}{4\pi d_u(t)}\right) \exp\left(\frac{-j2\pi d_u(t)}{\lambda_i}\right) \exp\left(-\frac{K(f_i)d_u(t)}{2}\right),$$

where $\lambda_i = \frac{c}{f_i}$, and $K(f_i)$ is the overall absorption coefficient of the transmission medium on sub-band $i$.[1]

### B. IRS-Assisted Transmission Links

The transmission vector from the UAV to the first element of the IRS is denoted as $\boldsymbol{r}_0(t) = \boldsymbol{l}_0 - \boldsymbol{l}(t) = [a - X(t), -Y(t), b - H]^T$. The difference vector from the $(n_x, n_z)$-th element of the IRS to the first element of the IRS is $\Delta\boldsymbol{r}_{n_x,n_z}(t) = [(n_x - 1)\delta_x, 0, (n_z - 1)\delta_z]^T$. Then, at time slot $t$, the relative phase difference on sub-band $i$ between the signal received at the first element and at the $(n_x, n_z)$-th element is $\theta^i_{n_x,n_z}(t) = \frac{2\pi \boldsymbol{r}_0(t)^T \Delta\boldsymbol{r}_{n_x,n_z}(t)}{\lambda_i r(t)}$, where $r(t) = |\boldsymbol{r}_0(t)|$. Then, the received array vector from UAV to the IRS at time $t$ on sub-band $i$ can be expressed as $\boldsymbol{e}_{i,r}(t) = [\exp(-j\theta^i_n(t))]^T$, $n = 1, \ldots, N$, where the subscript $n = n_z + (n_x - 1)N_z$.

The transmission vector from the first element of the IRS to UE $u$ is $\boldsymbol{r}_u = [(x_u - a), y_u, -b]^T$. Let $r_u = |\boldsymbol{r}_u|$. Then, at time slot $t$, the relative phase difference on sub-band $i$ between the signal that is reflected by the first element and by the $(n_x, n_z)$-th element to UE $u$ is $\vartheta^{i,u}_{n_x,n_z} = \frac{2\pi \boldsymbol{r}_u^T \Delta\boldsymbol{r}_{n_x,n_z}}{\lambda_i r_u}$. The transmit array vector from the IRS to UE $u$ at time $t$ on sub-band $i$ can be expressed as $\boldsymbol{e}_{i,u} = [\exp(-j\vartheta^{i,u}_n)]^T$, $n = 1, \ldots, N$, where the subscript $n = n_z + (n_x - 1)N_z$.

According to [11], in the far field scenario, the cascaded channel gain of the UAV-IRS-UE $u$ link on sub-band $i$ is

$$\tilde{g}_{i,u}(t) = \left(\frac{\lambda_i}{8\sqrt{\pi^3} r_u r(t)}\right) \exp\left(\frac{-j2\pi r^s_u(t)}{\lambda_i}\right) \exp\left(-\frac{K(f_i) r^s_u(t)}{2}\right),$$

where $r^s_u(t) = r(t) + r_u$. Then, the channel gain of the UAV-IRS-UE $u$ can be expressed as $g_{i,u}(t) = \tilde{g}_{i,u}(t)\boldsymbol{e}_{i,r}(t)\boldsymbol{\Phi}(t)\boldsymbol{e}_{i,u}{}^T$, where $\boldsymbol{\Phi}(t) = \text{diag}(\exp(j\phi_1(t)), \ldots, \exp(j\phi_N(t)))$, and $\exp(j\phi_n(t))$ represents the reflecting coefficient of the $n$-th reflecting element.

### C. Problem Formulation

Let $B_i$ denote the bandwidth of sub-band $i$, and the power spectral density of the noise in sub-band $i$ is denoted by $S_N(f_i)$. The obtained transmission rate of UE $u$ on sub-band $i$ in time slot $t$ is given by

$$R_{i,u}(t) = B_i \log\left(1 + \frac{p_i(t)|h_{i,u}(t) + g_{i,u}(t)|^2}{S_N(f_i)B_i}\right), \quad (1)$$

where $p_i(t)$ denotes transmit power on sub-band $i$ at slot $t$.

In this problem, we first consider the following constraints for the UAV's trajectory $\{\boldsymbol{l}(t)\}$ as

$$C1: \boldsymbol{l}(T) = \boldsymbol{l}(1) = \bar{\boldsymbol{l}}_1, \quad (2)$$

$$C2: |\boldsymbol{l}(t+1) - \boldsymbol{l}(t)| \le V_{max}\frac{T_s}{T}, t = 1, \ldots, T-1. \quad (3)$$

The constraint $C1$ indicates that UAV returns to its initial location by the end of $T_s$, and the initial location is fixed to $\bar{\boldsymbol{l}}_1$. The constraint $C2$ indicates that the maximum distance that the UAV can travel in each time slot is $V_{max}\frac{T_s}{T}$, where $V_{max}$ represent the maximum speed of the UAV.

Define the binary variable $\alpha_{i,u}$ to indicate whether UE $u$ transmits on sub-band $i$ or not. Assume that each sub-band is allocated to only one UE. Then, we have

$$C3: \alpha_{i,u} \in \{0,1\}, \sum_{u=1}^{U} \alpha_{i,u} = 1, i \in \mathcal{I}, u \in \mathcal{U}. \quad (4)$$

The transmit power is limited by maximum power $p_{max}$ as

$$C4: \sum_{i=1}^{I} p_i(t) \le p_{max}. \quad (5)$$

The phase shift of each reflecting element of the IRS varies within the range of $[0, 2\pi]$, we have

$$C5: 0 \le \phi_n(t) \le 2\pi, 1 \le n \le N. \quad (6)$$

[1]As the LoS paths are the most significant components of all channels (UAV-IRS, IRS-UEs, and UAV-UEs) in the considered scenario, the reflected paths contributed by scatterers in the ground can be neglected [10].

Then, the problem can be formulated as

$$\max_{\substack{\{p_i(t)\},\{\boldsymbol{l}(t)\}\\ \{\boldsymbol{\Phi}(t)\},\{\alpha_{i,u}\}}} \min_{u} R_u = \frac{1}{T}\sum_{t=1}^{T}\sum_{i\in\mathcal{I}}\alpha_{i,u}R_{i,u}(t) \quad (7)$$
$$\text{s.t.} \qquad C1-C5,$$

where $R_u$ represents the average rate of UE $u$. Our target is to maximize the minimum average rate among all UEs by jointly optimizing the UAV's trajectory, THz sub-band allocation, the phase shift of IRS and the power allocation. By introducing auxiliary variables $R_{th}$ and $\{H_{i,u}^t\}$, Problem (7) can be equivalently reformulated as

$$\max_{\mathcal{X}} \ R_{th} \quad (8a)$$
$$\text{s.t.} \ \frac{1}{T}\sum_{t=1}^{T}\sum_{i\in\mathcal{I}}\alpha_{i,u}B_iR_{i,u}^t(p_i(t),H_{i,u}^t)\geq R_{th}, u\in\mathcal{U}, \quad (8b)$$
$$|h_{i,u}(t)+g_{i,u}(t)|^2\geq\alpha_{i,u}H_{i,u}^t, i\in\mathcal{I}, u\in\mathcal{U}, \quad (8c)$$
$$C1-C5,$$

where $R_{i,u}^t(p_i(t),H_{i,u}^t)=\log(1+\frac{p_i(t)H_{i,u}^t}{S_N(f_i)B_i})$, and $\mathcal{X}\triangleq\{\{\boldsymbol{\Phi}(t)\},\{\alpha_{i,u}\},p_i(t),R_{th},\{H_{i,u}^t\},\{\boldsymbol{l}(t)\}\}$.

## III. Solutions

As the formulated problem (8) is non-convexity, we decouple the optimization into three subproblems: optimization of UAV's trajectory, optimization of the IRS's phase shift, the THz sub-band allocation and the power control problem.

### A. Trajectory Optimization

Given the sub-band allocation, the phase shift of IRS and power control, the UAV's trajectory is optimized in this subsection. The trajectory optimization is challenging due to the complicated expression of the overall channel gain as

$$\begin{aligned}H_{i,u}(\boldsymbol{l}(t)) &= |h_{i,u}(t)+g_{i,u}(t)|^2\\ &=\frac{A_i^2}{d_u^2(t)}\exp(-K_id_u(t))\\ &\quad+\frac{B_{i,u}^2}{r^2(t)}\exp(-K_ir(t))C_{i,u}^2(\boldsymbol{l}(t))\\ &\quad+\frac{2D_{i,u}(\boldsymbol{l}(t))}{d_u(t)r(t)}\exp\left(-\frac{1}{2}K_i(r(t)+d_u(t))\right),\end{aligned} \quad (9)$$

where $A_i$, $B_{i,u}$, $K_i$, $C_{i,u}(\boldsymbol{l}(t))$, and $D_{i,u}(\boldsymbol{l}(t))$ are given by

$$A_i=\frac{\lambda_i}{4\pi}, B_{i,u}=\left(\frac{\lambda_i}{8\sqrt{\pi^3}r_u}\right)\exp\left(-\frac{1}{2}K_ir_u\right), K_i=K(f_i),$$
$$C_{i,u}(\boldsymbol{l}(t))=|\boldsymbol{e}_{i,r}(t)\boldsymbol{\Phi}\boldsymbol{e}_{i,u}{}^T|^2, d_u^s(t)=r(t)+r_u-d_u(t)$$
$$D_{i,u}(\boldsymbol{l}(t))=A_iB_{i,u}\Re\left\{\exp\left(\frac{-j2\pi d_u^s(t)}{\lambda_i}\right)\boldsymbol{e}_{i,r}(t)\boldsymbol{\Phi}\boldsymbol{e}_{i,u}{}^T\right\}.$$

It is observed that $C_{i,u}(\boldsymbol{l}(t))$ and $D_{i,u}(\boldsymbol{l}(t))$ consist of many periodic cosine patterns with respect to the sub-bands and UE indexes, which make the channel gain given in (9) difficult to handle. However, according to $C2$, with a sufficiently short time slot, the change of UAV's locations in a time slot is very small. As a result, we can first regard $C_{i,u}(\boldsymbol{l}(t))$ and $D_{i,u}(\boldsymbol{l}(t))$ as constants, then the function of $H_{i,u}(\boldsymbol{l}(t))$ can be significantly simplified. Therefore, at a given location $\boldsymbol{l}'(t)=[X'(t),Y'(t),H]$, we define

$$C_{i,u}^{t'}\triangleq C_{i,u}(\boldsymbol{l}'(t)), D_{i,u}^{t'}\triangleq D_{i,u}(\boldsymbol{l}'(t)).$$

In addition, we define functions $f_i(x)=\frac{1}{x^2}\exp(-K_ix)$ and $q_i(x,y)=\frac{1}{xy}\exp(-\frac{K_i}{2}(x+y))$. Then, the channel gain in (9) can be approximated as

$$\begin{aligned}\hat{H}_{i,u}(\boldsymbol{l}(t)) &= A_i^2f_i(d_u(t))+C_{i,u}^{t'}B_{i,u}^2f_i(r(t))\\ &\quad+2D_{i,u}^{t'}q_i(d_u(t),r(t)).\end{aligned} \quad (10)$$

Then, by checking the second-order derivative of $f_i(x)$ with respect to $x$, we have $\frac{\mathrm{d}^2f_i(x)}{\mathrm{d}x^2}>0$. In addition, the Hessian matrix of $q_i(x,y)$ can be verified to be positive definite. As a result, $f_i(x)$ and $q_i(x,y)$ are convex functions with respect to $x$ and $(x,y)$, respectively.

Although the expression given in (10) is greatly simplified, (8c) are still non-convex constraints by substituting $|h_{i,u}(t)+g_{i,u}(t)|^2$ with $\hat{H}_{i,u}(\boldsymbol{l}(t))$ in (10). Then, the successive convex approximation (SCA) is adopted to reformulate constraint (8c) by utilizing the first-order Taylor approximations of $f_i(x)$ and $q_i(x,y)$. Define $d_u^{t'}\triangleq|\boldsymbol{l}'(t)-\boldsymbol{l}_u|$, $r^{t'}\triangleq|\boldsymbol{l}_0-\boldsymbol{l}'(t)|$. Then, constraint (8c) can be approximated as

$$\zeta_{i,u}^td_u^t+\psi_{i,u}^tr^t+const_{i,u}^t\geq\alpha_{i,u}H_{i,u}^t, \quad (11)$$

where

$$\zeta_{i,u}^t=\left(A_i^2\frac{\mathrm{d}f_i}{\mathrm{d}x}(d_u^{t'})+2D_{i,u}^{t'}\frac{\partial q_i}{\partial x}(d_u^{t'},r^{t'})\right). \quad (12)$$
$$\psi_{i,u}^t=\left(C_{i,u}^{t'}B_{i,u}^2\frac{\mathrm{d}f_i}{\mathrm{d}x}(r^{t'})+2D_{i,u}^{t'}\frac{\partial q_i}{\partial y}(d_u^{t'},r^{t'})\right) \quad (13)$$
$$\begin{aligned}const_{i,u}^t &= A_i^2f_i(d_u^{t'})+C_{i,u}^{t'}B_{i,u}^2f_i(r^{t'})+\\ &\quad 2D_{i,u}^{t'}q_i(d_u^{t'},r^{t'})-\psi_{i,u}^tr^{t'}-\zeta_{i,u}^td_u^{t'}.\end{aligned} \quad (14)$$

Note that the first-order derivatives of $f_i(x)$ and $q_i(x,y)$ utilized in (12) are respectively given by

$$\frac{\mathrm{d}f_i}{\mathrm{d}x}(x)=-\frac{K_ix+2}{x^3}\exp(-K_ix), \quad (15)$$
$$\frac{\partial q_i}{\partial x}(x,y)=\frac{-(\frac{K_i}{2}x+1)}{x^2y}\exp\left(-\frac{K_i}{2}(x+y)\right). \quad (16)$$

It is verified that $f_i(x)$ is a decreasing function with respect to $x$, and $q_i(x,y)$ is a decreasing function with respect to $x$ and $y$, respectively. Then, given $\boldsymbol{L}_{-t}=[\boldsymbol{l}(1),\ldots,\boldsymbol{l}(t-1),\boldsymbol{l}(t+1),\ldots,\boldsymbol{l}(T)]$, and a given reference location $\boldsymbol{l}'(t)$, the UAV's location $\boldsymbol{l}(t)=[X(t),\ Y(t),\ H]^T$ at time slot $t$ can be determined by solving the following optimization problem

$$\max_{\mathcal{X}_1} \ R_{th} \quad (17a)$$
$$\text{s.t.} \ \sum_{i\in\mathcal{I}}\alpha_{i,u}B_iR_{i,u}^t(p_i(t),H_{i,u}^t)+R_u^{-t}\geq TR_{th}, \quad (17b)$$
$$|\boldsymbol{l}(t)-\boldsymbol{l}_u|\leq d_u^t, u\in\mathcal{U}, \quad (17c)$$
$$|\boldsymbol{l}_0-\boldsymbol{l}(t)|\leq r^t, \quad (17d)$$
$$(11), C1, C2,$$

where $\mathcal{X}_1=\{\boldsymbol{l}(t),d_u^t,r^t,H_{i,u}^t\}$. The $\{d_u^t\}$ and $r^t$ are auxiliary variables, and $R_u^{-t}=\sum_{s\neq t}^{T}\sum_{i\in\mathcal{I}}\alpha_{i,u}R_{i,u}(s)$.

**Algorithm 1** Successive Convex Approximation With Rate Constraint Penalty (CAR)

Initialize the convergence precision $\boldsymbol{\varsigma}$, trajectory $\{\boldsymbol{l}(t)^0\}$ and the number of iterations $m = 0$.
**repeat**
  **for** $t = 1, \cdots, T$ **do**
    Initialize $\boldsymbol{l}'(t) = \boldsymbol{l}(t)^m$ and $\mathcal{U}_R = \mathcal{U}$;
    **repeat**
      Obtain $\hat{\boldsymbol{l}}(t)$ by solving Problem (17);
      Update $\mathcal{U}_R$, replace $R_u^{-t}$ with $\hat{R}_u^{-t}$ for all $u \in \mathcal{U}_R$;
    **until** $\mathcal{U}_R = \varnothing$ or Problem (17) is not feasible;
    **if** $\mathcal{U}_R = \varnothing$ **then**
      Update $\boldsymbol{l}(t)^m = \hat{\boldsymbol{l}}(t)$;
    **end if**
  **end for**
**until** $|\boldsymbol{l}(t)^{m+1} - \boldsymbol{l}(t)^m| \leq \boldsymbol{\varsigma}, \forall t$.

Problem (17) is a convex problem, and it can be readily solved by the standard solvers, such as the CVX. Note that Problem (17) is formulated to determine the UAV's location at the time slot *t*, so that UAV's trajectory can be obtained by solving a series of $T$ optimization problems.

However, note that the channel gain given in (10) is a simplified version of (9). Let $(\hat{\boldsymbol{l}}(t), \hat{H}_{i,u}^t)$ denote the optimal solution to Problem (17). According to (10), we have $\hat{H}_{i,u}^t \neq H_{i,u}(\hat{\boldsymbol{l}}(t))$, so that the constraint in (17b) may not be satisfied with $(\hat{\boldsymbol{l}}(t), H_{i,u}(\hat{\boldsymbol{l}}(t)))$. Define

$$\Delta_u = \sum_{i \in \mathcal{I}} \alpha_{i,u} B_i R_{i,u}^t(p_i(t), H_{i,u}(\hat{\boldsymbol{l}}(t))) + R_u^{-t} - TR_{th}, \quad (18)$$

which is utilized to indicate whether constraint (17b) is satisfied by the obtained $(\hat{\boldsymbol{l}}(t), \hat{H}_{i,u}^t)$.

If $\Delta_u < 0$, the obtained $(\hat{\boldsymbol{l}}(t), H_{i,u}(\hat{\boldsymbol{l}}(t)))$ degrades the average achievable rate $R_u$ of UE *u*. Let $\mathcal{U}_R$ denotes the set of UEs with $\Delta_u < 0$. To guarantee that $R_u \geq R_{th}$ for all UEs in $\mathcal{U}_R$, more strict constraints are introduced by defining

$$\hat{R}_u^{-t} = R_u^{-t} + \Delta_u, \forall u \in \mathcal{U}_R. \quad (19)$$

Correspondingly, constraint (17b) is updated by substituting $R_u^{-t}$ with $\hat{R}_u^{-t}$ for all $u \in \mathcal{U}_R$. Then, by continuously solving the updated Problem (17) with the modified rate constraints for the UEs in $\mathcal{U}_R$, the obtained solution $(\hat{\boldsymbol{l}}(t), H_{i,u}(\hat{\boldsymbol{l}}(t)))$ will not degrade the objective. However, it is worth pointing out that the updated problem may not be feasible, as the change of UAV's location in a time slot is very small due to constraint $C2$. In this case, no new UAV's position that can improve the current objective value $R_{th}$ can be found, i.e., the UAV should stay in the current position $\boldsymbol{l}'(t)$. Overall, the above analysis can be summarized as the following CAR Algorithm 1 to optimize the UAV's trajectory.

### *B. Phase Shift Optimization*

Given the THz sub-band allocation, the power control, and the UAV's trajectory, we first reformulate (9) as

$$|h_{i,u}(t) + g_{i,u}(t)|^2 = G_{i,u}(t) + F_{i,u}(t)|\boldsymbol{v}_{i,u}(t)\boldsymbol{\phi}(t)|^2 + \Re\{Q_{i,u}(t)\boldsymbol{v}_{i,u}(t)\boldsymbol{\phi}(t)\}, \quad (20)$$

where $G_{i,u}(t) = (\frac{A_i}{d_u(t)})^2 \exp(-K_i d_u(t))$, $\boldsymbol{\phi}(t) = \text{diag}(\boldsymbol{\Phi}(t))$, $\boldsymbol{v}_{i,u}(t) = [1, \ldots, \exp(-j(\vartheta_N^{i,u} + \theta_N^i(t)))]^T$, $F_{i,u}(t) = (\frac{B_{i,u}}{r(t)})^2 \exp(-K_i r(t))$, $d_u^s(t) = r(t) + r_u - d_u(t)$, and $Q_{i,u}(t) = \frac{2A_i B_{i,u}}{d_u(t) r(t)} \exp(-\frac{1}{2} K_i (r(t) + d_u(t)) - j2\pi \frac{d_u^s(t)}{\lambda_i})$.

Define $s_{i,u}(t) = \boldsymbol{v}_{i,u}(t)\boldsymbol{\phi}(t)$, and it is observed that the right hand side of (20) can be formulated as a convex function with respect to $s_{i,u}(t)$ as

$$U(s_{i,u}(t)) = G_{i,u}(t) + F_{i,u}(t) s_{i,u}(t) s_{i,u}^*(t) + \frac{1}{2} Q_{i,u}(t) s_{i,u}(t) + \frac{1}{2} Q_{i,u}(t)^* s_{i,u}^*(t). \quad (21)$$

Given $\tilde{s}_{i,u}(t) = \boldsymbol{v}_{i,u}(t)\tilde{\boldsymbol{\phi}}(t)$, we have

$$U(s_{i,u}(t)) \geq U(\tilde{s}_{i,u}(t)) + \Re\Big\{\Big(2F_{i,u}(t)\tilde{s}_{i,u}^*(t) + Q_{i,u}(t)\Big)(\boldsymbol{v}_{i,u}(t)\boldsymbol{\phi}(t) - \tilde{s}_{i,u}(t))\Big\}. \quad (22)$$

The phase shift of IRS can be optimized by solving a sequence of problems as

$$\max_{0 \leq \phi_n(t) \leq 2\pi} \quad R_{th} \quad (23a)$$

$$\text{s.t.} \quad \alpha_{i,u}(\Re\{\Upsilon_{i,u}(t)\boldsymbol{v}_{i,u}(t)\boldsymbol{\phi}(t)\} - \chi_{i,u}(t)) \geq 0, \quad (23b)$$

where $\Upsilon_{i,u}(t) = (2F_{i,u}(t)\tilde{s}_{i,u}^*(t) + Q_{i,u}(t))$ and $\chi_{i,u}(t) = \Re\{\Upsilon_{i,u}(t)\tilde{s}_{i,u}(t)\} - U(\tilde{s}_{i,u}(t)) + H_{i,u}^t$. Although Problem (23) is nonconvex, as proved in [4], its globally optimal solution can be found by the following procedure. First, a penalty is added in the objective with the pricing factors $\{\rho_i(t)\}$. Then, the phase shift can be determined by

$$\max_{0 \leq \phi_n(t) \leq 2\pi} \quad R_{th} + \sum_{i \in \mathcal{I}} \rho_i(t) \sum_{u=1}^{U} \alpha_{i,u}(\Re\{\Upsilon_{i,u}(t)\boldsymbol{v}_{i,u}(t)\boldsymbol{\phi}(t)\} - \chi_{i,u}(t)). \quad (24)$$

The solution to Problem (24) is given by

$$\phi_n(t) = \angle(\Xi_n(t)), \quad (25)$$

and $\Xi_n(t)$ is the *n*-th element of $\boldsymbol{\Xi}(t)$, which is

$$\boldsymbol{\Xi}(t) = \sum_{i \in \mathcal{I}} \rho_i(t)\alpha_{i,u}(\Re\Big\{\Upsilon_{i,u}^*(t)\boldsymbol{v}_{i,u}^*(t)\Big\}. \quad (26)$$

To reduce the penalty, pricing factors are updated by sub-gradient method. In the *s*-th iteration, $\rho_i(t)^{(s)}$ is updated as

$$\rho_i(t)^{(s)} = \left[\rho_i(t)^{(s-1)} - \tau_i(t)^{(s)}\left(\sum_{u=1}^{U} \alpha_{i,u} \nabla_{i,u}^{\rho}(t)\right)\right]^+ \quad (27)$$

where $\nabla_{i,u}^{\rho}(t) = \Re\{\Upsilon_{i,u}(t)\boldsymbol{v}_{i,u}(t)\boldsymbol{\phi}(t)\} - \chi_{i,u}(t)$, $[a]^+ = \max\{0, a\}$, and $\tau_i^{(s)}$ is the step-size in the *s*-th iteration.

### *C. THz Sub-Band Allocation and Power Control*

Given UAV's trajectory, and the phase shift of the IRS, the THz sub-band allocation and power control are optimized as

$$\max_{\alpha_{i,u}, R_{th}, p^i(t)} \quad R_{th} \quad (28a)$$

$$\text{s.t.} \quad \frac{1}{T}\sum_{t=1}^{T}\sum_{i \in \mathcal{I}} \alpha_{i,u} B_i R_{i,u}^t(p_i(t), H_{i,u}^t) \geq R_{th}, \quad (28b)$$

$$C3, C4.$$

**Algorithm 2** Algorithm to Solve Problem (8)

1: Initialize trajectory $\boldsymbol{l}^0(t)$, phase shift $\boldsymbol{\Phi}^0(t)$, convergence precision $\sigma$ and the number of iteration $m = 0$.
2: **repeat**
3: Calculate $\alpha_{u,i}^{(m+1)}$, $p_i(t)^{(m+1)}$, and $R_{th}^{(m+1)}$ by solving Problem (28);
4: Calculate $\{\boldsymbol{l}(t)^{(m+1)}\}$ according to CAR Algorithm;
5: Initialize precision $\boldsymbol{\theta}$, $\boldsymbol{\phi}(t)^{(0)} = \text{diag}(\boldsymbol{\Phi}(t)^m)$ and the number of iteration $n = 0$;
6: **repeat**
7: Obtain Problem (24) with $s_{i,u}(t)^n = \boldsymbol{v}_{i,u}(t)\boldsymbol{\phi}(t)^{(n)}$;
8: Calculate $\boldsymbol{\phi}(t)^{(n+1)}$ by solving Problem (24);
9: **until** $|\boldsymbol{\phi}(t)^{(n+1)} - \boldsymbol{\phi}(t)^{(n)}| \leq \boldsymbol{\theta}$;
10: Obtain $\boldsymbol{\Phi}(t)^{m+1}$ according to $\boldsymbol{\phi}(t)^{(n+1)}$;
11: **until** $|R_{th}^{(m+1)} - R_{th}^{(m)}| \leq \sigma$.

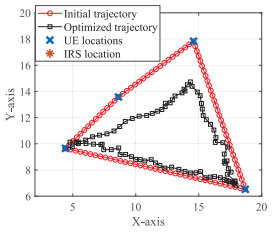


Fig. 2. Converged UAV's trajectory.

Introducing transformation $x_{u,i}(t) = \alpha_{u,i}p_i(t)$, the above Problem (28) can be solved by using the dual-based method given in [12].

In summary, based on the above analysis, we propose the following Algorithm 2 to solve the original Problem (8).

First, the solution generated by the CAR algorithm is always feasible to the original Problem (8), and $R_{th}^{(m+1)}$ is non-decreasing due to (19). Thus, the sequence of solutions generated by Algorithm 2 is always feasible for Problem (8). Furthermore, as Algorithm 2 is based on the block coordinate descent (BCD) method, the monotonic property of the generated solutions by Algorithm 2 can then be verified [9]. Thus, the convergence of Algorithm 2 is guaranteed.

## IV. Simulation Results

Simulation results are presented in this section to evaluate the proposed scheme. In our simulation, the transmission frequency range is 240-400 GHz, the bandwidth of sub-band is 20 GHz, and the molecular absorption coefficients are generated according to [13]. For the IRS, $b = 2$ m, $N_x = 8$, $N_z = 10$, and $\delta_x = \delta_z = 1$ mm. For the UAV, $H = 10$ m, $p_{max} = 1$ W, $V_{max} = 1$ m/s, $T_s = 1$ min, and $T = 100$. For comparison, we consider three different algorithms: 1) The sub-band allocation and power control are randomly selected during the iterations and labeled as "PwCh fixed"; 2) The phase shift of the IRS is randomly generated during the iterations and labeled as "Theta fixed"; 3) The trajectory of the UAV is fixed as the initialized one during the iterations and labeled as "Traject fixed."

Fig. 2 illustrates the optimized trajectory. It is observed that the optimized trajectory requires the UAV to move a much smaller distance than that of the initial trajectory, which is attributed to the jointly optimized phase shift of IRS, the THz channel allocation, and the power control. This also implies that UAV can save energy for the flight and the proposed algorithm fully exploits the benefit brought by the joint design of UAV's trajectory and IRS reflecting coefficients. Fig. 3 shows the minimum average rate of UEs obtained by different algorithms. It is observed that the proposed algorithm achieves the best performance. Moreover, the performance gaps between the proposed algorithm and the benchmarks are considerable and keep increasing with iterations, which verifies the effectiveness of the proposed algorithm.

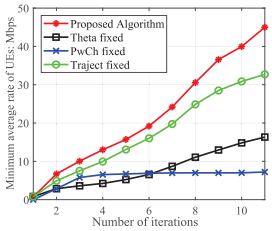


Fig. 3. Convergence performance.

## V. Conclusion

In this letter, the minimum average rate of UEs has been maximized by optimizing the UAV's trajectory, the phase shift of IRS, the THz sub-band allocation and the power control. The simulation results validated the effectiveness of the proposed algorithm.

## References

[1] Q. Wu, S. Zhang, B. Zheng, C. You, and R. Zhang, "Intelligent reflecting surface aided wireless communications: A tutorial," 2020. [Online]. Available: http://arxiv.org/pdf/2007.02759v2.
[2] C. Pan *et al.*, "Multicell MIMO communications relying on intelligent reflecting surfaces," *IEEE Trans. Wireless Commun.*, vol. 19, no. 8, pp. 5218–5233, Aug. 2020.
[3] C. Chaccour, M. N. Soorki, W. Saad, M. Bennis, and P. Popovski, "Risk-based optimization of virtual reality over terahertz reconfigurable intelligent surfaces," 2020. [Online]. Available: https://arxiv.org/pdf/2002.09052.
[4] Y. Pan, K. Wang, C. Pan, H. Zhu, and J. Wang, "Sum rate maximization for intelligent reflecting surface assisted terahertz communications," 2020. [Online]. Available: https://arxiv.org/pdf/2008.12246.
[5] S. Fang, G. Chen, and Y. Li, "Joint optimization for secure intelligent reflecting surface assisted UAV networks," *IEEE Wireless Commun. Lett.*, vol. 10, no. 2, pp. 276–280, Feb. 2021.
[6] M. Hua, L. Yang, Q. Wu, C. Pan, C. Li, and A. L. Swindlehurst, "UAV-assisted intelligent reflecting surface symbiotic radio system," 2021. [Online]. Available: https://arxiv.org/abs/2007.14029.
[7] J. M. Jornet and I. F. Akyildiz, "Channel modeling and capacity analysis for electromagnetic wireless nanonetworks in the terahertz band," *IEEE Trans. Wireless Commun.*, vol. 10, no. 10, pp. 3211–3221, Oct. 2011.
[8] H. Lu, Y. Zeng, S. Jin, and R. Zhang, "Aerial intelligent reflecting surface: Joint placement and passive beamforming design with 3D beam flattening," 2020. [Online]. Available: https://arxiv.org/pdf/2007.13295.
[9] Y. Yang, S. Zhang, and R. Zhang, "IRS-enhanced OFDMA: Joint resource allocation and passive beamforming optimization," 2019. [Online]. Available: https://arxiv.org/pdf/1912.01228.
[10] S. K. Moorthy and Z. Guan, "Flytera: Echo state learning for joint access and flight control in THz-enabled drone networks," in *Proc. IEEE Int. Conf. Sens. Commun. Netw. (SECON)*, 2020, pp. 1–9.
[11] W. Tang *et al.*, "Wireless communications with reconfigurable intelligent surface: Path loss modeling and experimental measurement," 2020. [Online]. Available: https://arxiv.org/pdf/1911.05326.
[12] C. Y. Wong, R. S. Cheng, K. B. Lataief, and R. D. Murch, "Multiuser OFDM with adaptive subcarrier, bit, and power allocation," *IEEE J. Sel. Areas Commun.*, vol. 17, no. 10, pp. 1747–1758, Oct. 1999.
[13] A.-A. A. Boulogeorgos, E. N. Papasotiriou, and A. Alexiou, "A distance and bandwidth dependent adaptive modulation scheme for THz communications," in *Proc. IEEE 19th Int. Workshop Signal Process. Adv. Wireless Commun.*, 2018, pp. 1–5.